Prediction of Electron Beam Depth of Penetration

Beam focus current was found to be the most critical factor in establishing depth of penetration

BY W. H. GIEDT AND L. N. TALLERICO

ABSTRACT. Analytical and experimental results showing the relationship between electron beam welding machine settings and penetration depth were reviewed. This led to the development of the following proposed equation for representing the relation between partial penetration and the independent variables involved in electron beam welding:

$$(P/dk_a\theta_m) = 3.33(vw/\alpha_a)^{0.625}$$

The dimensionless group on the left contains the ratio of the beam power P to penetration depth d multiplied by the average thermal conductivity k_a and the melting temperature above ambient θ_m. The dimensionless group on the right (vw/α_a) includes the effect of welding velocity v and fusion zone width at the surface w divided by the average thermal diffusivity α_a of the workpiece.

Data scatter was of the order of $\pm 40\%$ for values of $(vw/\alpha_a) < 1.0$, improving to around $\pm 20\%$ for $(vw/\alpha_a) > 10$. Estimates of the effects of possible deviations of machine settings from reported or optimum values were of the order of magnitude of the data scatter. Beam focus coil current deviation was found to have the greatest influence on predicted penetration. The priority for precision in machine settings was concluded to be the following: 1) optimum beam focus coil current, 2) beam voltage or current, 3) welding velocity, and 4) focus coil to work distance.

Introduction

Research studies have contributed substantially to an understanding of the electron beam (EB) welding process and to providing guidance in selecting appropriate welding conditions for specific tasks. However, test programs to determine machine settings to make a particular weld are still common. Since such testing may be costly and require considerable time (and may repeat previous work), a review of relevant analytical and experimental research was undertaken. The objectives were to develop relations between the fundamental variables which could be used to select machine settings or to focus and limit necessary field testing and to assess the relative importance of errors in individual welding variables.

Analytical and empirical approaches for determining the relationship between electron beam power and penetration and welding velocity were first reviewed. Attention was restricted to partial penetration. The procedure was first to consider how the EB welding process was modeled and to compare results predicted by the various models. Next, these results were compared with available experimental measurements. Although the data points fell around the analytical curves, they did not agree well with any particular curve over the range covered. Observation of the data suggested that they could be adequately represented by a single curve. An equation based on a least squares fitting program was determined. Corrections were then developed to account for the effects of nonoptimum focus coil current operation and for the distance between the focus coil and workpiece. The relative importance of errors or deviations in individual machine variables and workpiece thermal properties was investigated by evaluating the appropriate partial derivatives of this equation.

W. H. GIEDT is a Consultant and L. N. TALLERICO is Supervisor, Process Development and Fabrication Division, Sandia National Laboratories, Livermore, Calif.

KEY WORDS

Electron Beam Welding
Depth of Penetration
Partial Penetration
Electron Beam Power
Welding Velocity
Beam Focus Current
Focus Coil Current
Coil Work Distance
Power Depth Ratio
Fusion Zone Width

Analytical Models and Solutions

Basically, all models proposed for predicting partial penetration during electron beam welding utilize either the two-dimensional moving-line-source solution or the solution for a cylindrical or elliptical cavity moving through an infinite plate. In addition, dimensional analysis has been used to correlate experimental data.

Line Source Correlations

Hashimoto and Matsuda (Ref. 1) assumed a wedge-shaped molten volume with base (surface) dimensions equal to the EB width. They approximated the heat loss by conduction from the constant thermal property moving-line-source solution at the solid-liquid interface at a distance of one-half the beam diameter from the line source. This should be applicable at the surface, but would be expected to be less accurate with increasing distance below the surface since the fusion zone decreases with depth. The acceptable agreement of the theory with low-voltage welding machine measurements, however, suggests that the approximations made were appropriate. The heat balance analysis presented by Lupin (Ref. 2) was similar to that of Ref. 1 and yielded correct order of magnitude predictions of high-voltage welding.

A different approach in applying the moving-line-source solution is described by Swift-Hook and Gick in Ref. 3. They assumed that the melting temperature isotherm determined the location (and shape) of the liquid-solid interface. For a uniform power input P along a line source of length d (the penetration), the moving-line-source solution gives the temperature distribution in cylindrical coordinates r and ϕ as

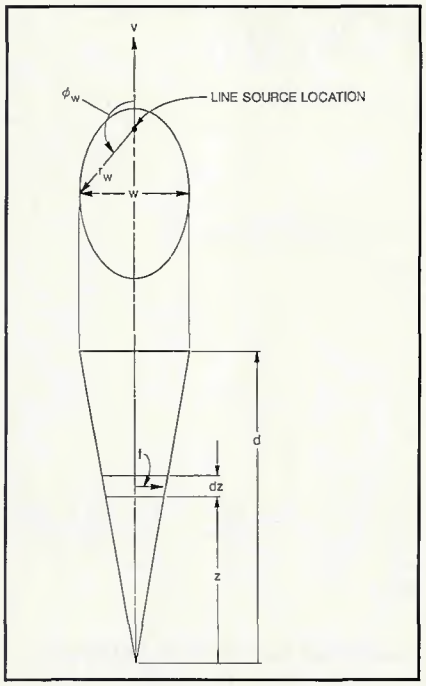

Fig. 1—Schematic of conically shaped fusion zone

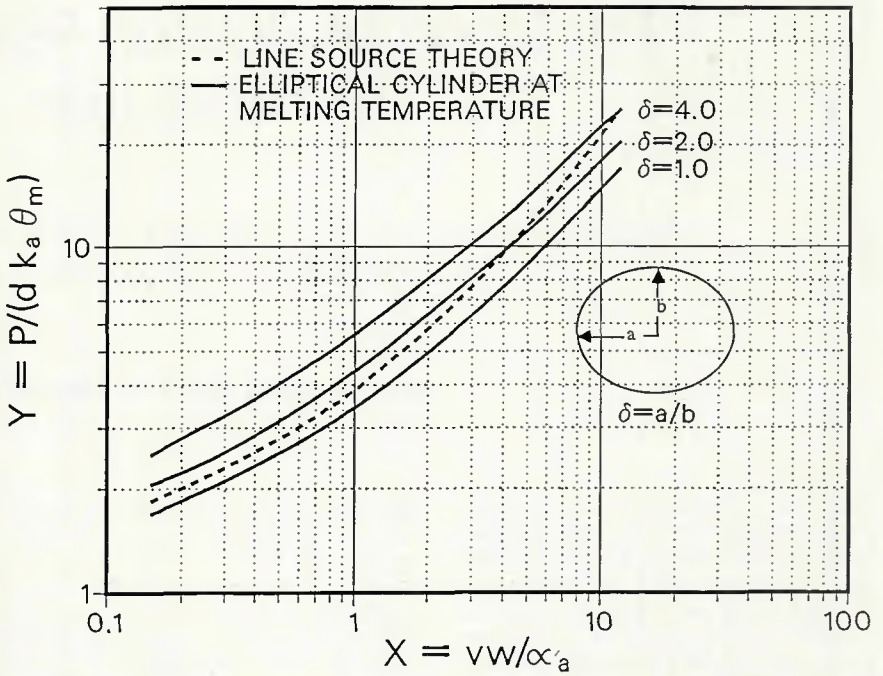

Fig. 2—Power-to-depth ratio variation with welding velocity based on moving-line-source and elliptical cavity solutions

$$(T-T_o)/(T_m-T_o) = (P/d)/[2\pi k(T_m-T_o)]\exp\{-(vr/2\alpha)\cos\phi\}K_o(vr/2\alpha) \quad (1)$$

With $T = T_m$, the relation for the locus of the melting isotherm is then

$$(P/d)/(2\pi k\theta_m) = \exp\{(vr/2\alpha)\cos\phi\}/K_o(vr/2\alpha) \quad (2)$$

in which $\theta_m = T_m - T_o$. At the maximum width w of the melting isotherm, the relation between the radius r_w and angle ϕ_w (Fig. 1) defining this location is

$$\cos\phi_w = K_o(vr_w/2\alpha)/K_o'(vr_w/2\alpha) \quad (3)$$

The half-width of the fusion zone w/2 is thus:

$$w/2 = r_w\sin\phi_w = r_w[1 - K_o\{(vr_w/2\alpha)/K_o'(vr_w/2\alpha)\}^2]^{1/2} \quad (4)$$

The value of r_w for a given w can be determined from this equation and substituted in Equation 2 to obtain P/d for specified material properties k and α and welding velocity v.

Explicit relations for the power input per unit depth of penetration were derived in Ref. 3 for low and high welding velocity regions. However, iterative solution of Equations 2 and 4 to determine values of P/d for specified material properties and welding velocity can be easily carried out with a small computer. This solution is plotted (dashed line) in Fig. 2 in terms of $(P/d)/k_a\theta_m$ and (vw/α_a) where the subscript a indicates that thermal properties would be evaluated at an average temperature, normally $T_m/2$.

Fig. 3—Schematic of electron beam welding

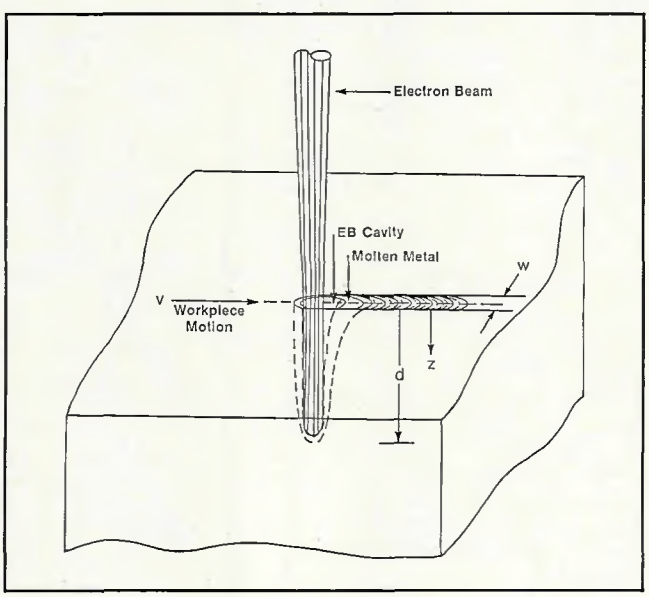

Moving Elliptical Cavity Solution

The moving-line-source solution is based on quasi-steady heat flow by conduction from a line at which the temperature approaches infinity. In the actual welding process, however, the intense beam creates a vapor-filled cavity, as illustrated in Fig. 3. Energy from the beam is deposited in the liquid surrounding this cavity and transferred to the liquid-solid interface by convection. During deep penetration EB welding, the cross-section defined by the outer boundary of the molten metal can be approximated by a cylinder, elliptical in shape. Since this surface must be at the melting temperature, an alternate approach has been to calculate the quasi-steady heat transfer rate from elliptical cylinders moving with constant speed in an infinite plate (Ref. 4). Predicted variations of power per unit depth $(P/d)/k_a\theta_m$ for ellipse axes ratios of $\delta = 1$, 2 and 4 are presented in Fig. 2. In this figure, elliptical cylinder dimensions and source strength (*i.e.*, P/d) are constant in the depth direction.

Note that the curve from the moving-line-source solution moves from the $\delta = 1.0$ curve across the $\delta = 2.0$ and eventually above the $\delta = 4.0$ curves as the parameter vw/α_a increases. This indicates that the liquid-solid interface changes from cylindrical to an elongated ellipse with increasing welding speed.

In both the moving-line-source and elliptical cylinder solutions, a dimensionless distance $(1/2)\ vr/\alpha$ occurs. Note that $X = vw/\alpha_a$ is simply the same combination of variables with the 1/2 omitted for simplicity. The dimensionless quantity $Y = P/(dk_a\theta_m)$ is also readily developed from either the line source or cylindrical cavity solutions. The depth is placed in the denominator instead of the numerator so that the trend of the curves is upward to the right.

Dimensional Analysis Correlation

The correlation presented by Hablanian (Ref. 5), which was developed by applying dimensional analysis, uses essentially the same variables as in Fig. 2. The only significant differences are: 1) a fictitious melting temperature is introduced, which accounts for the heat of fusion; and 2) the length dimension in the vw/α_a variable is the EB diameter. Although acceptable correlation of data was shown in Ref. 5, no information is given about thermal properties used and how EB diameter was determined or defined. Since an EB diameter is difficult to determine, and the dimensions of fusion zone are generally important in specifying weld parameters, use of the latter quantity was considered preferable.

Comparison of Theoretical Curves with Experimental Data

In comparing theory with experiment, it is essential to specify clearly how the individual quantities involved are determined. X and Y include thermal properties that vary substantially over the temperature ranges encountered. Also, the fusion zone width varies from a maximum (normally at the surface) to zero at the root or base. Common practice is to evaluate the thermal conductivity and thermal diffusivity at some mean temperature between ambient and melting, commonly $T_m/2$. Unfortunately, specifying the temperature at which to evaluate these properties may not be sufficient because reported data may not agree or data may not be available. For this reason, it is considered essential to list values used in plotting experimental points. For alloys, the recommended value for the melting temperature is the average between the solidus and liquidus temperatures. EB weld fusion zones normal to the welding direction tend to be triangular in shape (illustrative transverse cross-sections are shown in Fig. 4). The logical value for w is the width at the surface. However, there are two characteristics of transverse EB fusion zones that must be considered in determining or specifying w. The first is the occurrence of a "nail head" at the top of the weld. The second is that, for sharply focused beams, the fusion zone width may be almost constant over half or more of the depth (*e.g.*, Fig. 4C). To account for these characteristics, it is proposed that w be defined as the width at the base of a triangle, which has approximately the same cross-sectional area as the fusion zone.

Data for aluminum and steel, for which fusion zone profiles are available, have been plotted in Fig. 5 using the definitions given above. Thermal property values used are listed in Table 1. The curves shown for comparison are for a conically shaped fusion zone. They have been determined from the results in Fig. 2 (where P/d is constant) by integrating from the base (where $w = 0$) to the surface where the width = w. Note that this results in lower values of $P/(dk_a\theta_m)$ than in Fig. 2 for the same values of vw/α_a. The details of the analytical procedure are given in Appendix B for a moving-line source model and in Ref. 4 for the elliptical cavity model.

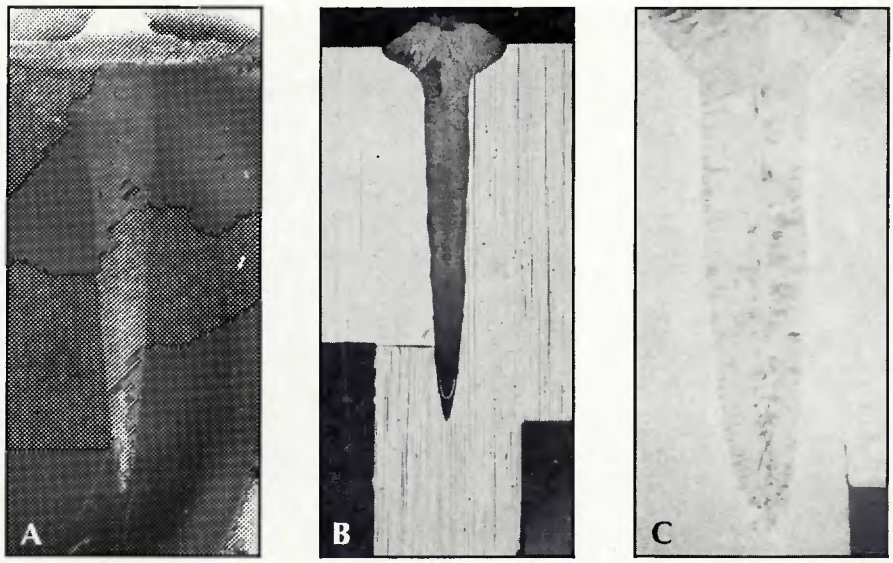

Fig. 4 — Transverse sections of electron beam welds in 304 stainless steel. A — Beam voltage 32 kV, beam current 155 mA, welding velocity 0.5 cm/s, focused at surface (ribbon filament); B — beam voltage 100 kV, beam current 13 mA, welding velocity 1.27 cm/s, focused at surface (ribbon filament); C — beam voltage 116 kV, beam current 16 mA, welding velocity 0.631 cm/s, focused below surface

Table 1—Average Thermal Property Values Used[a]

Material	Melting Range T_s °C	Melting Range T_ℓ °C	$T_m = \frac{(T_\ell + T_s)}{2}$ °C	$\theta_m = T_m - T_o$, $T_o = 20°C$ °C	$T_a = \frac{T_o + T_m}{2}$ °C	k_a W/cm°C	α_a cm²/s
Al 1100	643	657	650	630	325	2.10	0.780
Al 2024	502	638	570	550	285	1.75	0.670
Al 6061	582	649	616	596	308	1.40	0.670
Carbon steel	1530		1530	1510	755	0.20	0.055
Stainless steel 304	1400	1455	1428	1408	714	0.25	0.045
En 58J (~SS316)	1400	1450	1425	1405	712	0.25	0.046

(a) Based on data given by Y. S. Touloukian, R. W. Powell, C. Y. Ho and P. G. Klemens in *Thermophysical Properties of Matter*, Vols. 1 and 10, IFI/Plenum, N.Y., 1970, Ref. 10.

Most of the data points in Fig. 5 in the lower range of X (from 0.15 to 2.0) fall within the range of the moving elliptical cavity curves for axis ratios of 1 to 4. At the high values of X, the data fall near or above the $\delta = 4$ curve. This is consistent with the expected trend toward an increasingly elongated melt isotherm with increasing welding velocity. Factors such as small workpiece size, joint geometry and thermal properties differing from values employed may also contribute to the scatter.

Empirical Equation for Partial Penetration

Noting that the data in Fig. 5 do not agree well with any of the theoretical curves, it was decided to investigate the

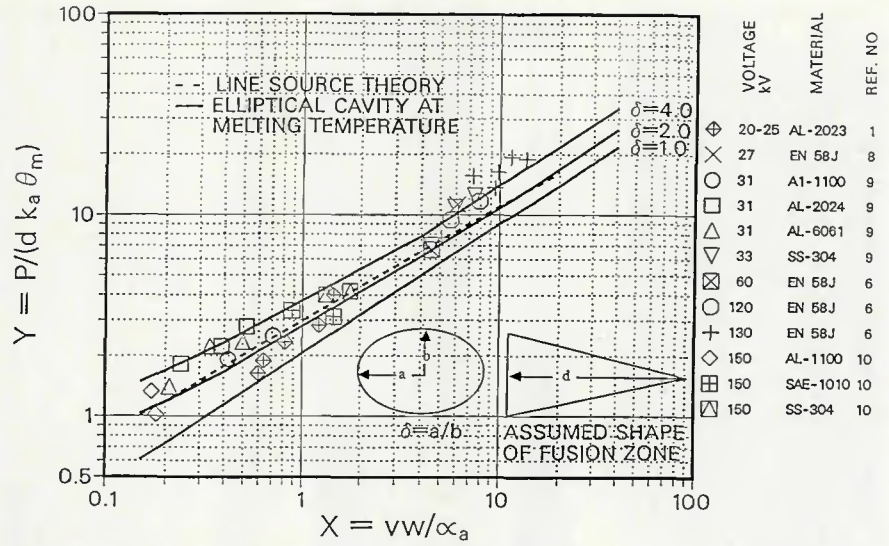

Fig. 5 – Comparison of measured with predicted EBW penetration

possibility of correlating the points with a power curve of the form $Y = aX^b$. A least squares fitting program yielded the following equation:

$$Y = 3.33\ X^{0.625} \qquad (5)$$

This is shown along with the data in Fig. 6. The coefficient of determination (the fraction of the variation in the dependent variable which has been accounted for in the fit) is 0.955. In view of the data scatter, a simple relation such as this appears to be acceptable. The factors which may account for the variations in Fig. 6 are investigated in the following section.

Effects of Deviations or Errors in Machine Variables

Beam Focus Coil Current

The data presented in Fig. 5 or Fig. 6 are for the beam focused to produce maximum penetration. This is usually achieved with the beam focused at or slightly below the workpiece surface. Referring to this condition as the optimum focus current (OFC), the effect of operation at nonoptimum conditions was investigated by Adams (Ref. 6) who reported that the change in penetration depends on the beam voltage and current. At lower penetrations and lower power, there is a tendency for the fusion zone to broaden with nonoptimum beam focus, and for penetration to decrease relatively more than for deeper penetration and higher power. He also notes that the sensitivity of the depth/width ratio decreases with increasing distance of the focus coil to the workpiece, WD. These trends are consistent with results presented by Engquist (Ref. 7) who emphasized that it was best to operate at the shortest possible focus coil to work distance. The reason for this is illustrated in Fig. 7, where it can be seen that curves are very steep for focus coil to beam focal point locations greater than 4 in. (10 cm). Hence, in this region, a small error in focus coil current can cause a significant change in the effective focal point of the beam. This trend is due to the fact that the focal distance of a beam from the focus coil, FD, varies as

$$FD = CV/(FC)^2 \qquad (6)$$

where V is the beam voltage, FC is the focus coil current, and C is a proportionality constant.

Study of the results presented in Ref. 6 suggested that when considered on a percentage basis, the effect of nonoptimum focus coil current was related to beam power. To account for this effect, it is proposed to multiply the right hand side of Equation 5 by the following term:

$$[1 + K(FCD)]^{0.625} \qquad (7)$$

Here, K denotes a constant which will depend on the voltage, focus coil current and the machine being used. FCD denotes the deviation of the focus coil current FC from the optimum focus coil current OFC; *i.e.*, $FCD = |FC - OFC|/OFC$. For a fixed power input, the general effect of operation at nonoptimum beam focus current is a decrease in penetration and an increase in the width of the fusion zone. Note that by raising the quantity in brackets in Equation 7 to the 0.625 power, the effect when $FCD > 0$ can be regarded as an increase in w. That is,

$$(vw/\alpha_a)^{0.625}[1 + K(FCD)]^{0.625} = (vw[1 + K(FCD)]/\alpha_a)^{0.625} \qquad (8)$$

Effectively, the variable X is increased; this increases Y which is due to a decrease in d for a fixed power level.

Decreases in the d/w ratio reported in Ref. 6 were from 2–10% for a 1% deviation of FC from OFC. Hence, the factor K in Equation 7 will have a value of between 2.0 and 10.0. Values of FCD will generally be between 0.01 and 0.05.

A more fundamental representation of the influence of beam focus coil current than is given by Equation 8 would require detailed information about the effect of voltage and work distance for a particular machine. This is beyond the scope of the present study. Here, the objective was to point out the importance of the focus coil

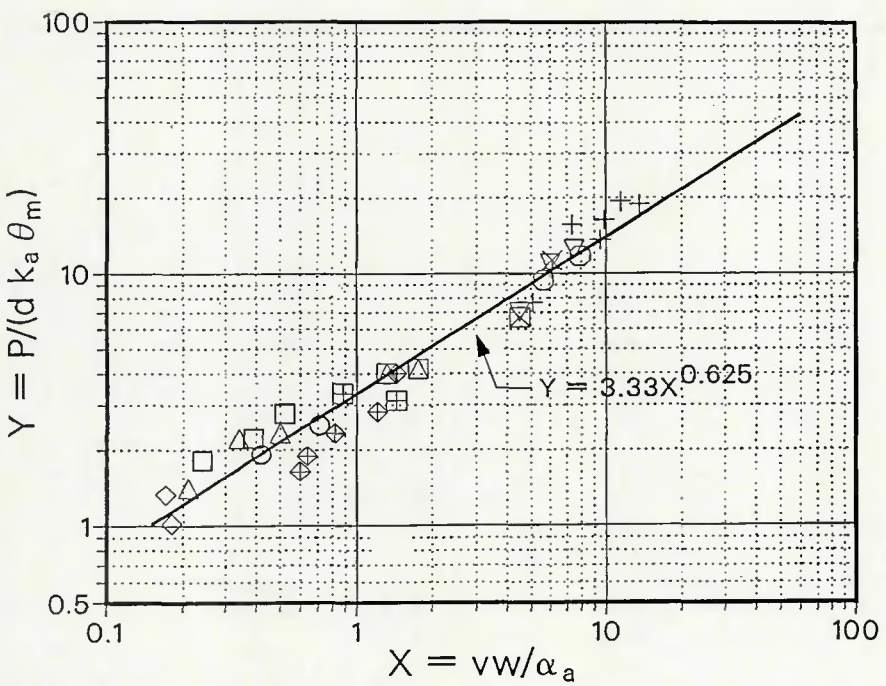

Fig. 6 – Correlation of EBW partial penetration data

current and the order of magnitude of the deviation in penetration which can result from nonoptimum focus coil current operation.

Effect of Focus Coil to Workpiece Distance

Within practical working distances (up to 4-6 in./10-15 cm) for a low-voltage welding machine and 9-10 in. (22.5-25.0 cm) for high-voltage welding machines, limited results indicate that optimum penetration decreases slightly with increasing distance between focus coil and workpiece. Using the approximate value of 4% per in. given by Adams (Ref. 8) for the rate of change, the magnitude of this effect was included in Equation 5 by dividing the right-hand side by the term

$$[1 - 0.04(WD - WD_{min})] \qquad (9)$$

where WD_{min} is a minimum working distance and WD is an actual working distance, both measured in inches.

The final dimensionless equation for the power per unit of penetration is, therefore,

$$\frac{(P/d)}{k_a\theta_m} = \frac{3.33(vw/\alpha_a)^{0.625}[1+K(FCD)]^{0.625}}{[1-0.04(WD-WD_{min})]} \qquad (10)$$

Estimates of the Effects of Independent Variable Deviations on Penetration

The sensitivity of penetration to errors or deviations in welding parameters can be estimated by expressing d as the dependent variable and differentiating with respect to each of the independent variables.

$$d = \frac{VXI[1-0.04(WD-WD_{min})]}{3.33\ k_a\theta_m(vw/\alpha_a)^{0.625}[1+K(FCD)]^{0.625}} \qquad (11)$$

with independent machine variables of V, I, v, FCD and WD.

Expressions for the partial derivatives of d with respect to V, I, v, FCD and WD are given in Ref. 9. The relative effects of an error or deviation in each of the welding variables were evaluated for the two cases specified in Table 2.

Low and high values of the parameter X (0.5 and 10.0) were selected for investigation of possible errors due to deviations in machine settings. These are designated as Case I and Case II in Table 2, which also includes representative values of V, I, v and WD characteristic of X = 0.5 and 10.0.

Estimated variations in penetration due to 5% deviations in machine settings were calculated for the two cases listed in Table 2. The results are summarized in Table 3.

Note that the total estimated errors is on the order of 25%. Referring to the comparison of the individual contributions shown on the right side of Table 3, it is seen that the beam focus current is the most critical machine parameter and that work distance is the least important. The variation in penetration is from 2 to 3 times more sensitive to deviations (errors) in the beam focus location than to deviations in voltage or current.

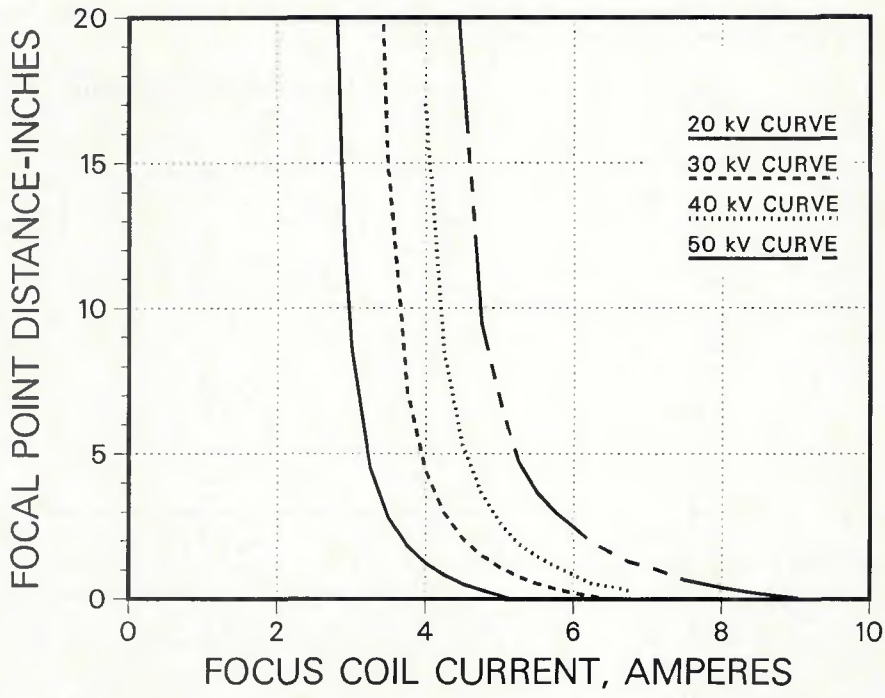

Fig. 7—Effect of focus coil current on distance from focus coil to beam focal point (Ref. 7)

Effects of Incorrect Average Thermal Properties

Workpiece thermal properties generally vary substantially over welding temperature ranges. Also, property values may be influenced by alloying-element concentration variations and by the material's processing history. From a practical point of view, such property variations are accounted for by the selection of appropriate average values. Comparison of measured with predicted temperatures indicates this approach to be acceptable. The relative importance of possible deviations of the average thermal properties selected can also be estimated from Equation 11. Penetration is indicated to vary inversely with the first power of the average thermal conductivity k_a and directly with the 0.625 power of the thermal diffusivity α_a. However, since $\alpha = k/\rho c$, α depends on k. To separate these two properties it is reasonable to consider $\alpha_a = k_a/(\rho c)_a$, *i.e.*, as a ratio of the average thermal conductivity k_a and the average thermal capacity $(\rho c)_a$. The penetration is then found to be proportional to the −0.375 power of the average thermal conductivity and to the −0.625 power of the average thermal capacity. That is:

$$d \propto k_a^{-0.375}\,(\rho c)_a^{-0.625} \qquad (12)$$

Differentiating this relation with respect to k_a and $(\rho c)_a$ and expressing deviations

Table 2—Representative Welding Conditions

Case	vw/α_a	V kV	I A	v cm/s	WD in.
I	0.5	100	0.012	0.5	6
II	10.0	150	0.040	1.5	6

Table 3—Errors in Penetration Due to 5% Deviations in Machine Settings (%)

Case	Total Error $\frac{\Delta d}{d}$	Percentage Contributions of Individual Parameters $\frac{\partial d}{\partial V}\Delta V$	$\frac{\partial d}{\partial I}\Delta I$	$\frac{\partial d}{\partial u}\Delta v$	$\frac{\partial d}{\partial (FCD)}\Delta FCD$	$\frac{\partial d}{\partial (WD)}\Delta WD$
I	25	19.8	19.8	12.4	43.1	4.8
II	22	15.3	15.3	14.3	49.6	5.5

Table 4—Data from Welds Made in 304 Stainless Steel

Weld	Beam Voltage kV	Beam Current mA	Weld Velocity cm/s	Heat Shield to Work in.	Weld Width at Surface cm	Depth of Penetration Measured-d_m cm	Depth of Penetration Predicted-d_p cm	Deviation $(d_p - d_m)/d_m$ %
				Machine A				
End	100	12.0	1.27	6	0.152	0.457	0.410	−10.0
Girth	100	5.0	1.27	6	0.114	0.228	0.206	−10.0
				Machine B				
Tube-to-valve	100	2.0	0.94	6	0.107	0.091	0.103	13.4
Plug	100	6.0	1.27	6	0.135	0.368	0.222	−40.0
Plunger	132	0.90	1.92	6	0.056	0.056	0.056	5.0
				Machine C				
Cap-body	115	21.0	1.55	6	0.119	0.643	0.853	33.0
Shell-body	96	16.0	1.63	6	0.074	0.526	0.707	35.7

as above shows that the effect on d of errors of Δk_a and $\Delta(\rho c)_a$ is $\Delta d/d = -0.375(\Delta k_a/k_a) - 0.625\Delta(\rho c)_a/(\rho c)_a$. Hence errors of 5% in k_a and $(\rho c)_a$ would affect d by ±1.9% and ±3.2%, respectively. These effects are noted to be less than those for similar percentage deviations in focus coil current, voltage or current, but similar in magnitude to the influence of welding velocity deviations.

Comparison with Recent Stainless Steel Welds

To test the applicability of the proposed relation, predicted penetrations for welds made with high-voltage welding machines were compared with measured values. Welding conditions and results are summarized in Table 4.

Referring to Table 4, it is seen that 4 out of 7 predicted penetrations are within 15% of the measured values. The predicted penetrations for the two welds made with Machine C are 30–35% higher than measured values. Such differences could be due to deviations from indicated welding parameters, particularly the beam focus current reading. The plug weld made with Machine B is interesting in that the measured penetration is 40% greater than predicted. Note that the beam voltage and current settings for the girth weld made with Machine A were similar in magnitude, while the penetration was over 50% less. This difference is similar to the magnitude of the data scatter in Fig. 6 and illustrates the substantial variations observed in current operation.

Conclusions

Experimental results for power per unit penetration during EB partial penetration welding were compared with predictions based on the moving-line-source and constant-temperature elliptical cavity solutions. The independent variable included the welding velocity times the weld width at the surface divided by the average thermal diffusivity of the material. Although the experimental trend was predicted, the data did not agree well with any of the analytical curves. In view of this, a simple logarithmic relation that represented the data within ±40% was determined. The applicability of this result was verified by comparison with measured penetrations of recent welds made in stainless steel.

The effects of possible deviations or errors in machine settings and average thermal properties were estimated from the partial derivatives of the empirical equation determined for the penetration. For the cases studied, the beam focus current was found to be the most critical parameter, and the distance between the focus coil and workpiece the least important. The variation in penetration is from 2 to 3 times more sensitive to deviations (errors) in beam focus current setting than to errors in beam voltage or current. Thus, the priority for obtaining accurate results should be: 1) optimum beam focus current, 2) beam voltage or current, 3) welding velocity, and 4) focus coil to work distance. The effects of incorrect average thermal property values were estimated to be of the same magnitude as the effect of a similar percentage deviation in welding speed.

References

1. Hashimoto, T., and Matsuda, F. 1965. Effect of welding variables and material upon bead shape in electron beam welding. *Trans. National Research Institute for Metals* 7(3):22-35.

2. Lupin, B. T. 1966. *A Correlation of Electron Beam Welding Parameters.* ASME Paper 66-WA/MET-18.

3. Swift-Hook, D. T., and Gick, A. E. R. 1973. Penetration welding with lasers. *Welding Journal* 52(11):492-s to 499-s.

4. Miyazaki, T., and Giedt, W. H. 1982. Heat transfer from an elliptical cylinder moving through an infinite plate applied to electron beam welding. *Int. J. Heat and Mass Transfer* 25(6):807-814.

5. Hablanian, M. H. 1963. A correlation of welding variables. *Proc. 5th Electron and Ion Beam Symposium.* Edited by J. R. Morely, Alloyed Electronics, Cambridge, Mass., pp. 262-268.

6. Adams, M. J. 1968. High voltage electron beam welding. *British Welding Journal* 57:451-467.

7. Engquist, R. D. 1968. Parameters affecting electron beam welding. *Metals Engineering Quarterly* 8(1):56-63.

8. Adams, M. J. 1963. Low voltage electron beam welding: effect of process parameters. *British Welding Journal* 52:134-142.

9. Giedt, W. H. 1986. *Prediction of Electron Beam Welding Depth of Penetration.* Report No. SAND86-8205, Sandia National Laboratories, Livermore, Calif.

10. Touloukian, Y. S., Powell, R. W., Ho, C. Y., and Klemens, P. G. 1972. *Thermophysical Properties of Matter,* Vols. 1 and 10, Plenum Publishing Corp., New York, N.Y.

Appendix A

Nomenclature

- c = Specific heat capacity of workpiece
- d = Depth of penetration
- I = Beam current
- k = Thermal conductivity
- K_o = Modified Bessel function of second kind and zero order
- K_o' = First derivative of K_o
- P = Beam power
- r = Radial distance from line source
- T = Temperature
- v = Welding velocity
- V = Beam voltage
- w = Transverse width of fusion zone at surface
- α = Thermal diffusivity
- δ = Ratio of ellipse major and minor axes
- ϕ = Angle measured from travel direction
- ρ = Density of workpiece
- θ = Temperature measured above ambient

Subscripts

a = Evaluated at one-half the melting temperature
m = Melting temperature
o = Ambient temperature
w = At maximum transverse width of fusion zone

Appendix B

Calculation of Penetration from Moving-Line-Source Solution for a Conically Shaped Fusion Zone

To account for the effect of the decrease in fusion zone width with depth during partial penetration EB welding, the liquid-solid interface can be approximated as a conical surface elongated in the welding direction—Fig. 1. For typical welds, the fusion zone is relatively deep and narrow (values of d/w of 5 or greater are common). Because of this, heat transfer in any plane parallel to the surface is primarily two-dimensional; *i.e.*, the heat transfer in the depth direction is negligible. If it is then assumed that the moving-line-source solution is applicable, the temperature distribution in any thin layer, a distance z from the bottom of the fusion zone, is specified by introducing the maximum width 2f of the melt isotherm at that location in the moving-line-source solution. This is accomplished by changing the parameter $(vr_w/2\alpha)$ in Equation 1 to $(vf/2\alpha)(r_w/f)$. Then for $(T - T_o)/(T_m - T_o) = 1.0$, Equation 1 for a thin layer dz becomes

$$dP = [2\pi k_a\theta_m \exp[(vf/2\alpha)(r_w/f)\cos\phi_w]/K_o[(vf/2\alpha)(r_w/f)]dz \quad (A1)$$

in which ϕ_w and f are related by

$$\cos\phi_w = K_o[(vf/2\alpha)(r_w/f)]/K_o'[(vf/2\alpha)(r_w/f)] \quad (A2)$$

The total power required for welding to a depth d is obtained by integrating Equation A1 from z = 0 to z = d. Setting

$$(vf/2\alpha)(r_w/f) = W, \quad (A3)$$

$$P = 2\pi k_a\theta_m \int_o^d \exp\{WK_o(W)/K_o'(W)\}/K_o(W)]dz \quad (A4)$$

Since the half width at z is f = (z/d)(w/2), df = (w/2d)dz and Equation A4 can be expressed as

$$P = 2\pi k_a\theta_m (2d/w) \int_o^{w/2} [\exp\{WK_o(W)/K_o'(W)\}/K_o(W)]\,df \quad (A5)$$

This result is next nondimensionalized by introducing $(2v/\alpha_a)$:

$$P/(dk_a\theta_m) = (4\pi/w)/(2v/\alpha_a)\int_o^{vw/\alpha_a} [\exp\{WK_o(W)/K_o'(W)\}/K_o(W)(2v/\alpha_a)]df \quad (A6)$$

or

$$P/(dk_a\theta_m) = 2\pi/(vw/\alpha_a)\int_o^{vw/\alpha_a} [\exp\{WK_o(W)/K_o'(W)\}/K_o(W)]d(2vf/\alpha_a) \quad (A7)$$

To determine $P/(dk_a\theta_m)$ as a function of (vw/α_a), it is first necessary to solve Equation A2 for a series of values of $W = (vr_w/2\alpha_a)$ corresponding to the values of $(2vf/\alpha_a)$. This requires a trial and error procedure. With these results Equation A7 can be integrated numerically. The result is shown as the dashed curve in Fig. 5.

WRC Bulletin 331
February 1988

This Bulletin contains two reports prepared by the Japan Pressure Vessel Research Council (JPVRC) Subcommittee on Pressure Vessel Steels. The reports are involved with the variation in toughness data for weldments in pressure vessel steel structures.

Metallurgical Investigation on the Scatter of Toughness in the Weldment of Pressure Vessel Steels—Part I: Current Cooperative Research

This report covers the background of current cooperative research from 1973 to the present, covering 137 references on toughness and toughness testing of weldments.

Metallurgical Investigation on the Scatter of Toughness in the Weldment of Pressure Vessel Steels—Part II: Cooperative Research

The objective of this report was to investigate the variation in toughness of multipass weldments in a welded joint.

Publication of these reports was sponsored by the Subcommittee on Thermal and Mechanical Effects on Materials of the Welding Research Council. The price of WRC Bulletin 331 is $28.00 per copy, plus $5.00 for postage and handling. Orders should be sent with payment to the Welding Research Council, 345 E. 47th St., Suite 1301, New York, NY 10017.

WRC Bulletin 332
April 1988

This Bulletin contains two reports that characterize the mechanical properties of two different structural shapes of constructional steels used in the pressure vessel industry.

(1) Characteristics of Heavyweight Wide-Flange Structural Shapes
By J. M. Barsom and B. G. Reisdorf

This report presents information concerning the chemical, microstructural and mechanical (including fracture toughness) properties for heavyweight wide-flange structural shapes of A36, A572 Grade 50 and A588 Grade A steels.

(2) Data Survey on Mechanical Property Characterization of A588 Steel Plates and Weldments
By A. W. Pense

This survey report summarizes, for the most part, unpublished data on the strength toughness and weldability of A588 Grade A and Grade B steels as influenced by heat treatment and processing.

Publication of this Bulletin was sponsored by the Subcommittee on Thermal and Mechanical Effects on Materials of the Pressure Vessel Research Committee of the Welding Research Council. The price of WRC Bulletin 332 is $20.00 per copy, plus $5.00 for postage and handling. Orders should be sent with payment to the Welding Research Council, Suite 1301, 345 E. 47th St., New York, NY 10017.

WRC Bulletin 333
May 1988

Bibliography on Fatigue of Weldments and Literature Review on Fatigue Crack Initiation from Weld Discontinuities
By C. D. Lundin

The bibliography together with a review of the present state of assessment of the factors which affect fatigue crack initiation make up this document. The bibliography was compiled through the efforts of many students at The University of Tennessee utilizing the previously available bibliographies and computer searches.

Publication of this report was sponsored by the Subcommittee on Failure Modes in Pressure Vessel Components of the Materials and Fabrication Division of the Pressure Vessel Research Committee of the Welding Research Council. The price of WRC Bulletin 333 is $20.00 per copy, plus $5.00 for postage and handling. Orders should be sent with payment to the Welding Research Council, Suite 1301, 345 E. 47th St., New York, NY 10017.